PARTS OF THE ORIGINAL DOCUMENT

ARE OF POOR REPRODUCTIVE QUALITY

CERTAINES PARTIES DU DOCUMENT ORIGINAL

SONT DE PIÈTRE QUALITÉ DE REPRODUCTION

28438 DUP.

IGM88TC-301-668-G
CNRC 28438

ZINC NICKEL COATINGS FOR IMPROVED ADHERENCE AND CORROSION RESISTANCE

B. Arsenault, B. Champagne, P. Lambert, S. Dallaire

INDUSTRIAL MATERIALS RESEARCH INSTITUTE

National Research Council Canada

75 De Mortagne

Boucherville, Quebec, Canada, J4B 6Y4

ZINC-NICKEL COATINGS FOR IMPROVED ADHERENCE AND CORROSION RESISTANCE

B. ARSENAULT, B. CHAMPAGNE, P. LAMBERT and S. DALLAIRE
Industrial Materials Research Institute
National Research Council Canada
75 De Mortagne, Boucherville, Québec, Canada J4B 6Y4

SUMMARY

In-service plasma-sprayed ceramic coatings may spall catastrophically because corrosion products are developed at the coating-substrate interface. This phenomenon is likely to occur for ceramic coatings on steel substrates even when the substrates have first been coated with metallic bond coats. This work was aimed at developing zinc-nickel thermal-spray powders for cathodic protection of steel substrates. Powders were produced from zinc-30 wt% nickel alloy with a particle size distribution of 90-150 μm and a study of their spraying parameters on steel substrates was carried out. The performance of these zinc-nickel coatings was determined by subjecting plasma-sprayed alumina and chromia coatings with and without a zinc-nickel underlayer to aqueous corrosion for various periods of time according to the ASTM B117-85 test. The effect of degradation by corrosion was measured by the ASTM C633-79 procedure.

A drastic loss of bond strength was noticed for ceramic coatings deposited directly on steel substrates as a function of corrosion time. A similar behavior was also observed for ceramic coatings plasma-sprayed onto nickel-chromium bond coat. Results of electrochemical, salt-spray and bond strength tests pointed out that zinc-30 wt% nickel coatings provide a cathodic protection. This cathodic protection confers an active corrosion protection to the substrate and is not affected by the presence of porosity in the ceramic coating. The adhesion strength of these zinc-30 wt% nickel coatings is in the neighbourhood of 40 MPa.

INTRODUCTION

Modern technology has created a considerable demand for materials which possess adequate mechanical strength with good wear or corrosion resistance. A viable economic solution consists in the application of high performance coatings. Many research studies have been carried out to solve corrosion problems of several plasma-sprayed coatings in aggressive conditions [1-6]. Bond coats have been developed to significantly increase the performance and the reliability of coating systems. On an historical basis, the development of bond coat materials began with molybdenum in the early 1940 s and evolved to nickel-chromium alloys, to nickel-aluminum composites, to aluminum-bronze and to pre-alloyed nickel aluminum. All these bond coat materials have been primarily developed to increase the adherence of coatings and in some cases to provide also a good oxidation resistance but have not been really designed for protecting parts against aqueous corrosion in a humid environment. In aqueous environments, plasma-sprayed ceramic coatings used with commercial bond coat tend to lose their initial adhesive strength and may spall catastrophically with the growth of corrosion products at the coating-substrate interface.

This work was aimed at studying a bond coat that would give an active protection to steel substrates and a good anchoring for any subsequent layers. Zinc is well recognized for its cathodic protection effectiveness in comparison with other metals. But its high vapor pressure above the melting point and its sticking properties make it difficult to spray in

dense and adherent coatings. To overcome these difficulties, a novel zinc-nickel alloy that would have a higher melting point and low vaporization during plasma spraying, has been developed. This type of alloy should result in high density coatings having good adherence and good aqueous corrosion resistance. More attention was focused on the 70 wt% Zn, 30 wt% Ni alloy and on the effect of plasma spray deposition parameters to gain optimal adherence. The corrosion resistance of the zinc-nickel coatings as top coat or as an underlayer beneath Al_2O_3 and Cr_2O_3 was determined.

MATERIAL AND EXPERIMENTAL PROCEDURES

Two oxide powders (Cr_2O_3, $Al_2O_3.TiO_2$) and two metal alloy powders (NiCr, ZnNi) were plasma sprayed on carbon steel (SAE 1010) substrates. All the powders with the exception of the ZnNi alloy powder were commercially available. These powders whose chemical composition and particle size range are shown in Table I were plasma sprayed by using two spraying units: Plasmadyne and Bay State. Before being sprayed, substrates were grit blasted with 0.8-1.2 mm diameter corundum particles at a 350 MPa pressure.

The 70 wt% Zn - 30 wt% Ni alloy was prepared by melting zinc and nickel at a temperature of 1050°C under a slight argon pressure. After cooling, the ingot alloy was crushed to produce powder having a particle size ranging from 90 to 150 μm. This preparation procedure is required to obtain a powder with good flowability and to ensure dense and adherent plasma-sprayed coatings.

A composite powder made by the agglomeration of zinc and nickel particles is not expected to give satisfactory coatings, because of the large difference in melting temperature of zinc and nickel and the low boiling temperature of zinc. Therefore, an alloyed powder is required to avoid excessive vaporization during spraying.

Six different types of coatings were studied: Cr_2O_3, $Al_2O_3.TiO_2$, Zn.Ni, Cr_2O_3/NiCr, Cr_2O_3/ZnNi, $Al_2O_3.TiO_2$/ZnNi. Steel specimens to be coated consisted of 2.54 cm diameter cylindrical studs normally used to measure the bond strength. Coated on one end, these pieces were exposed to the severe environment of a salt spray cabinet according to the ASTM B-117-85 standard method. This corrosion test consists of a salt spray exposure of specimens for various periods of time. The maximum period of exposure used in this work was 1000 hours. This test has been chosen because corrosion conditions can be accurately reproduced.

In order to assess the extent of corrosion damage, measurements were done on specimens with increasing periods of corrosion exposure. The adhesion bond strength was determined according to the ASTM (C-633-79) standardmethod. Cross-sections of coatings were examined metallographically to identify the type of fracture (adhesive, cohesive, mixed) and the corrosion products.

Corrosion potential measurements were carried out with a Keithley (Model 616) high impedance electrometer on as-deposited coatings.

Specimens were covered with a drop of 3.5 wt% NaCl aqueous solution and measurements were done with a saturated calomel reference electrode, thirty (30) minutes after the immersion to allow the system to reach a steady state.

RESULTS AND DISCUSSION

Figures 1 and 2 show the physical appearance and the particle size distribution of the prealloyed ZnNi powder used in this study. It is noteworthy that fine particles can induce an excessive vaporization during spraying which is detrimental for the coating properties and consequently a narrow particle size distribution was used. great care has been done to select a narrow particle size distribution. Table II summarizes the spraying efficiency and the coating bond strength obtained with different spraying parameters. The corresponding metallographic cross-sections of the ceramic and the ZnNi coatings are shown in Figures 3 to 8.

The damaging effects of aqueous corrosion on plasma-sprayed coatings can be assessed by measuring their bond strength as a function of the corrosion time. Indeed the variation in bond strength is quite informative on their susceptibility to corrosion attack. Two types of bond strength-corrosion time dependence are generally expected. When no corrosion is present, the coating bond strength should remain constant with exposure time. For substrate-coating combination susceptible to corrosion, a sharp transition from high to low bond strength would be observed.

Figure 9a) illustrates the effect of corrosion exposure time on the bond strength of ZnNi coating. Unexpectedly, the bond strength is increased with exposure time and remains well above the initial value after 1000 hours. This surprising behaviour is partly explained by the absence of corrosion products on the surface and at the interface after the test as illustrated in Figure 9b). It is also likely related to the modification of the internal stresses distribution within the coating by the formation of zinc corrosion products.

Figures 10a) and 11a) illustrate the variation in bond strength of Cr_2O_3 and duplex Cr_2O_3/NiCr coatings. These two coatings behave similarly: since there is an initial period when the bond strength remains almost constant. This plateau is followed by a rapid decrease within a short interval of time. The onset of this transition in the bond strength is earlier for Cr_2O_3 than for Cr_2O_3/NiCr. These two coatings exhibit negligible bond strength which is equivalent to spalling conditions after 1000 hours exposure. As indicated in Figures 10a), 11a) the decrease of the bond strength of these coatings is associated with a change in their rupture mode. The as-sprayed Cr_2O_3 and Cr_2O_3/NiCr coatings exibited a pure cohesive rupture within Cr_2O_3 . This cohesive rupture mode changes to an adhesive rupture mode with the formation of corrosion products at the substrate/coating interface. The corrosion products found at the interface are red rust (ferrite, Fe_2O_3) and some black oxide (likely magnetite, Fe_3O_4). The formation of Fe_2O_3 and Fe_3O_4 is in accordance with the Pourbaix diagram [8].

The presence of these corrosion products was detected before that a significant decrease of the bond strength was observed. Ferrite (Fe_2O_3) was found at the surface of the Cr_2O_3 coating only within the first 100 hours during which period the bond strengths was almost constant.

At the beginning of the corrosion test, many corrosion sites are initiated at the contact zones between the electrolyte and the substrate through the open porosity. These corrosion sites are very active, uniformly dispersed and contiguous to the surface of the coating. Because the density of the corrosion products is much less than the density of steel, a large volume expansion occurs. Therefore, the formation of corrosion products at these sites leads to protrusion of Fe_2O_3 through the Cr_2O_3 or Cr_2O_3/NiCr coatings. As mentioned earlier, during this initiation period the bond strength is not yet affected. As the corrosion process progresses, the corrosion sites grow to form a continuous layer of corrosion products between the coating and the substrate (Figures 10b and 11b). Therefore, the onset of the transition in the bond strength corrosion exposure time dependence is related to the formation of the corrosion products at the substrate-coating interface. The use of a NiCr underlayer with Cr_2O_3 does not provide a barrier against aqueous corrosion. Figures 10a) and 11a) indicate no significant difference between those two coatings. The NiCr underlayer seems only to delay the decay in bond strength.

The corrosion resistance of Cr_2O_3/ZnNi (Figure 12a) is superior to that of Cr_2O_3/NiCr (Figure 11a). No corrosion products (Figure 12b) are observed for the Cr^2O^3/ZnNi coating after 1000 hours of salt spray

exposure. This result indicates that a ZnNi underlayer is very effective for protecting a steel substrate against corrosion by cathodic protection of the substrate. This intrinsic cathodic protection character is confirmed from electrochemical potential measurements of the coating. The ZnNi coating 70 wt% Zn, 30 wt% Ni, has a stable potential of -760/ECS in comparison with -550 mV/ECS for the grit-blasted steel substrate. This electrochemical potential of ZnNi provides the capability to effectively protect the steel substrate by sacrificial protection.

It is worth mentioning that the ZnNi coating cathodically protects substrates without the drawbacks associated with corrosion protection by passivation. Indeed it has been observed that substrate materials like stainless steel that are protected by passivation in aqueous environment are corroded at the substrate-coating interface by differential aeration cells [4]. A differential aeration cell is a corrosion mechanism related to the joint action of an aqueous environment and oxygen contained in the atmosphere reaching the substrate through the open pores present in the coating. This differential cell breaks the passivation causes the dissolution of Fe ion from the stainless steel and induces the formation of red rust (Fe_2O_3) at the interface and on the coating surface.

The ZnNi underlayer provides the same degree of protection when used with other types of ceramic coatings. This is illustrated here with a $Al_2O_3.TiO_2$ coating as shown in Figure 13a) and 14a). When there is no ZnNi underlayer, the same rapid decay in bond strength occurs with

exposure time as was observed with Cr_2O_3. A significant amount of corrosion products was formed at the interface (Figure 13b) after 1000 hours exposure in the salt spray cabinet. On the contrary when a ZnNi underlayer was deposited beneath the $Al_2O_3.TiO_2$ coating, no corrosion products could be observed after the salt-spray test (Figure 14b). The coating bond strength improves with the exposure time (Figure 14a) to reach a threefold improvement after 1000 hours. The electrochemical potentials of $Al_2O_3.TiO_2$ and substrate are -280 mV and -550 mV/ESC respectively. Here again, the ZnNi underlayer causes a cathodic protection with its -760 mV/ECS potential.

CONCLUSION

This work has demonstrated the effectiveness of a ZnNi alloy coating to protect a carbon steel substrate when used as bond coat or top coat. Plasma sprayed ceramic coatings like Cr_2O_3 and $Al_2O_3.TiO_3$ deposited on steel without a Zn-Ni underlayer were susceptible to corrosion attack. They displayed a sharp transition from their initial bond strengths to lower bond strengths with corrosion exposure time. The use of a Zn-Ni coating underlayer provides corrosion protection to the substrate which can then resist attack by chemically active ions passing through pores, such as Cl ions in salt water. Furthermore, it provides protection against corrosion mechanisms such as differential aeration cells that are related to the porosity and to the existence of galvanic cells, features that in turn are related to the material of the top coating.

REFERENCES

(1) R.A. Sulit, F. West, S.L. Kullerd. Proceedings of the National Thermal Spray Conference, ASM, Orlando, Florida, U.S.A., Sept. 1987, p.241.

(2) O. Knotek, R. Elsing, H.R. Heintz. Surface coating and Technology, 30 (1987) 107.

(3) A. Raman, G. Nnaike, A. Choudhury, C.R. Das. Corrosion Science, 25 (1985) 107.

(4) Y. Arata, A. Ohmori, J. Morimoto, J. Kudoh, M. Kishida, Osaha, Kinki. Proc. 10th Int. Thermal Spraying Conf., Essen, Germany, 2-6 May 1983, p.197.

(5) Y. Arata, A. Ohmori, G. Zhou, J. Xue. Transactions of Japanese Welding Research Institute, 13 (1984) 27.

(6) Y. Arata, A. Ohmori, G. Zhou, J. Xue, G. Li. Transactions of Japanese Welding Research Institute, 13 (1984) 107.

(7) G.M. Egert, Corrosion-NACE, 44 (1988) 36.

(8) M. Pourbaix, "Atlas of Electrochemical Equilibria in Aqueous Solutions", NACE, Houston, Texas, U.S.A., 2nd Edn., 1974, p.312.

Table 1 - **CHEMICAL COMPOSITION OF POWDERS**

	CHEMICAL COMPOSITION (wt%)			
	Cr_2O_3	$Al_2O_3 \cdot TiO_2$	NiCr	ZnNi
Al_2O_3	-	87.2	-	-
C	-	-	.02	-
Cr	.08	-	19.46	-
Cr_2O_3	98.4	-	-	-
Fe	-	-	.40	-
Fe_2O_3	-	-	-	-
Ni	-	-	79.22	30
Mn	-	-	0.4	-
Si	-	-	.76	-
SiO_2	.03	.02	-	-
TiO_2	.03	12.83	-	-
Zn	-	-	-	70
Particle size (µm)	+15-53	+15-53	+15-53	+90-150

Table 2 - **SPRAYING PARAMETERS AND BOND STRENGTHS**

Material	Plasmadyne Unit			Bay State Unit	
	ZnNi	Cr_2O_3	Al_2O_3/TiO_2	ZnNi	Cr_2O_3
Primary gas argon (l/m)	20	69	50	64	35
Secondary gas Helium (l/m)	78	13	24	-	-
Carrier gas argon (l/m) helium	6	6	6	7.6	5.7
Current (A)	200	1200	900	450	700
Voltage (V)	52	37	37	33	42
Powder Feed Rate g/m	37	24	15	28	21
Spraying Dist. (cm)	7	9	7	7	10
Gun speed (cm/s)	30	50	50	30	30
Efficiency %	60	30	56	60	30
Bond strength (MPa)	35	15	28	40	18

LEGEND TO FIGURES

Figure 1 - Scanning electron micrograph of the Zn-30 wt% nickel prealloyed powder.

Figure 2 - Particle size distribution of Zn-30 wt% nickel powder.

Figure 3 - As sprayed Cr_2O_3 coating .

Figure 4 - As sprayed $Al_2O_3.TiO_2$ coating.

Figure 5 - As sprayed Cr_2O_3/NiCr coating.

Figure 6 - As sprayed ZnNi coating.

Figure 7 - As sprayed Cr_2O_3/ZnNi coating.

Figure 8 - As sprayed Al_2O_3/ZnNi coating.

Figure 9a) - Bond strength of the Zn-30 wt% nickel coating as a function of the corrosion time.

Figure 9b) - Metallographic cross-section of the Zn-30 wt% nickel coating after 1000 hours of salt spray exposure.

Figure 10a) - Bond strength of the Cr_2O_3 coating as a function of the corrosion time.

Figure 10b) - Metallographic cross-section of the Cr_2O_3 coating after 1000 hours of salt spray exposure.

Figure 11a) - Bond strength of the Cr_2O_3/NiCr coating as a function of the corrosion time.

Figure 11b) - Metallographic cross-section of the Cr_2O_3/NiCr coating after 1000 hours of salt spray exposure.

Figure 12a) - Bond strength of the Cr_2O_3/ZnNi coating as a function of the corrosion time.

Figure 12b) - Metallographic cross-section of the Cr_2O_3/ZnNi coating after 1000 hours of salt spray exposure.

Figure 13a) - Bond strength of the $Al_2O_3.TiO_2$ coating as a function of the corrosion time.

Figure 13b) - Metallographic cross-section of the $Al_2O_3.TiO_2$ coating after 1000 hours of salt spray exposure.

Figure 14a) - Bond strength of the $Al_2O_3.TiO_2$/ZnNi coating as a function of the corrosion time.

Figure 14b) - Metallographic cross-section of the $Al_2O_3.TiO_2$/ZnNi coating after 1000 hours of salt spray exposure.

Figure 1 - Scanning electron micrograph of ZnNi prealloyed powder.

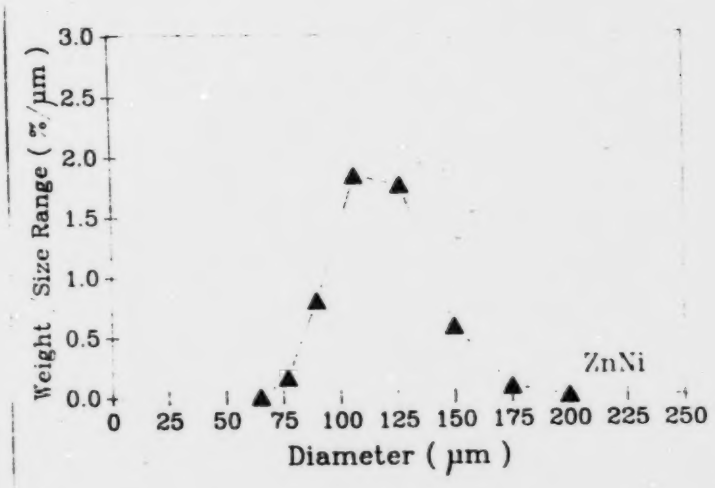

Figure 2 - Particle size distribution of ZnNi powder.

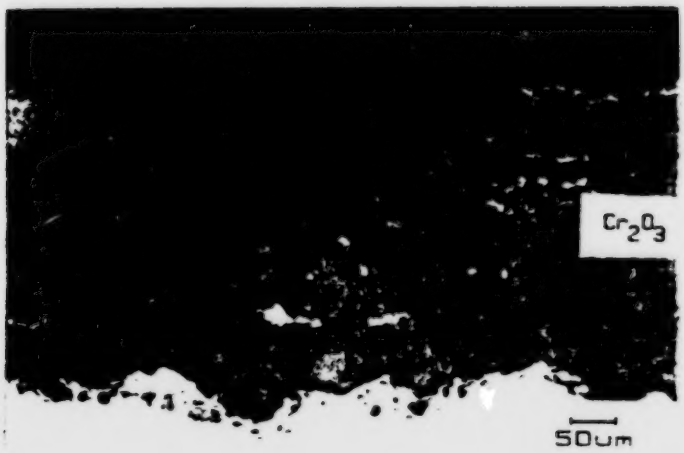

Figure 3 - Cr_2O_3 coating as sprayed.

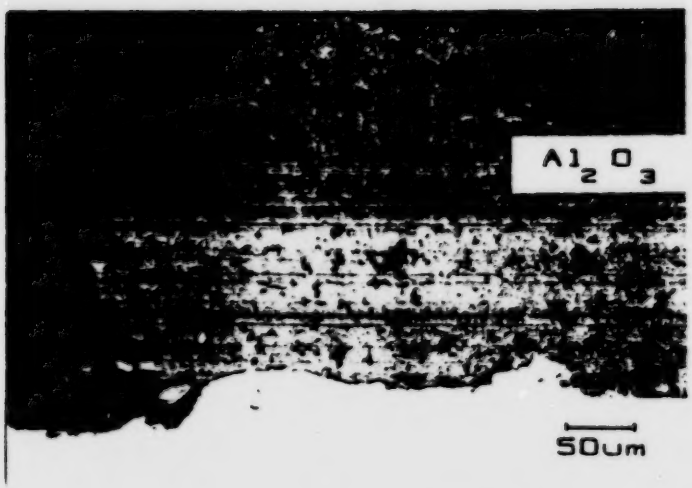

Figure 4 - $Al_2O_3.TiO_2$ coating as sprayed.

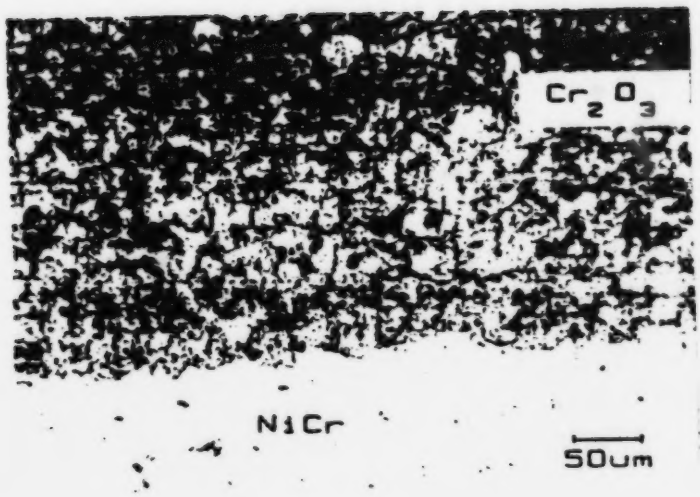

Figure 5 - Cr_2O_3/NiCr coating as sprayed.

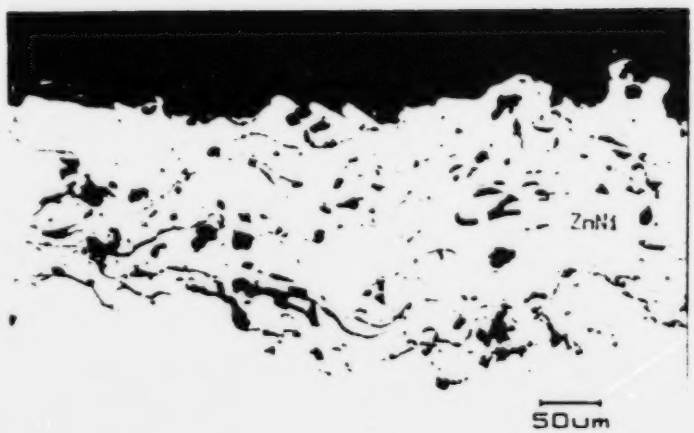

Figure 6 - ZnNi coating as sprayed.

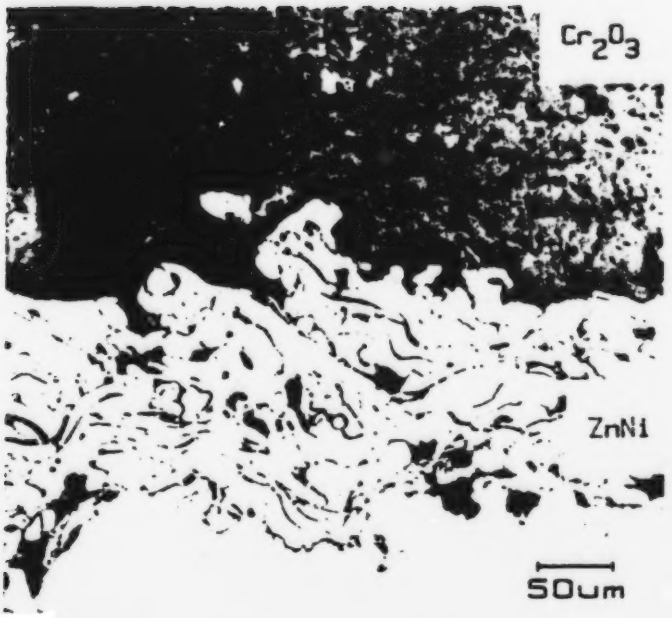

Figure 7 - Cr_2O_3/ZnNi coating as sprayed.

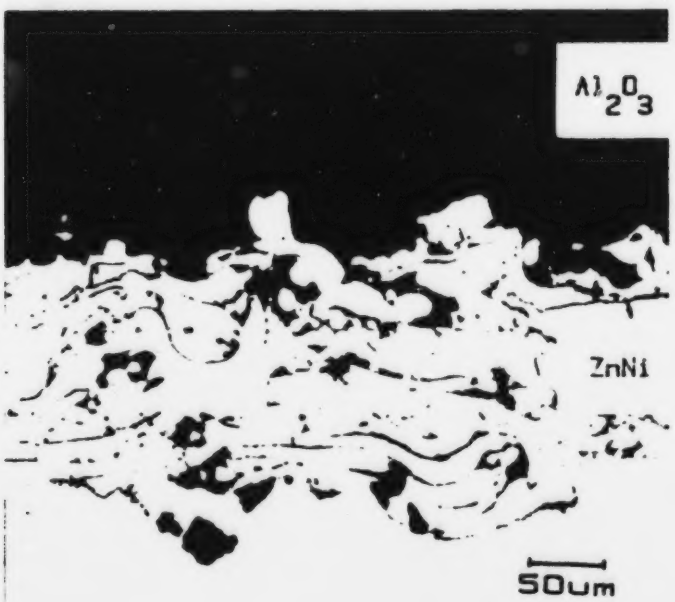

Figure 8 - Al_2O_3/ZnNi coating as sprayed.

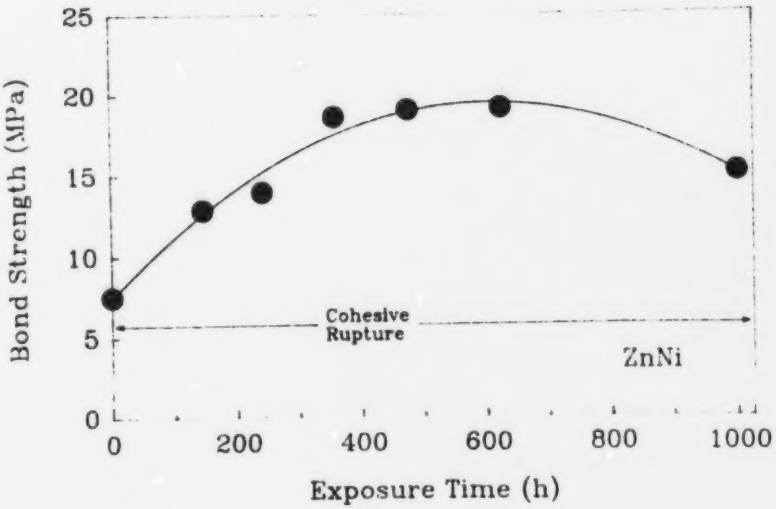

Figure 9a) - Bond strength of ZnNi coating as a function of corrosion time.

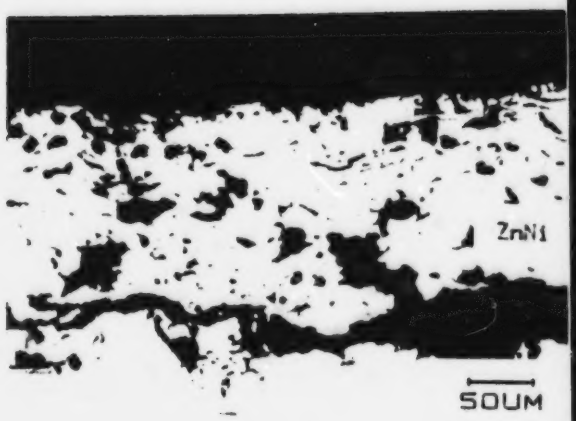

Figure 9b) - Metallographic cross-section of ZnNi coating after 1000 hours of salt spray exposure.

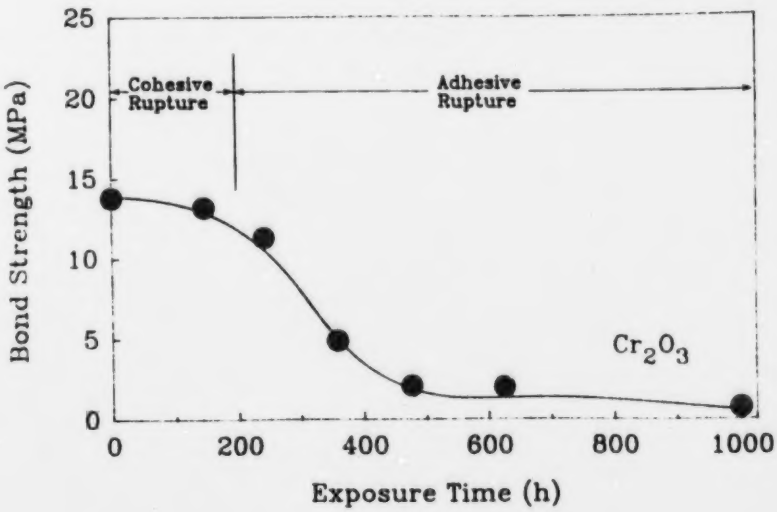

Figure 10a) - Bond strength of Cr_2O_3 coating as a function of corrosion time.

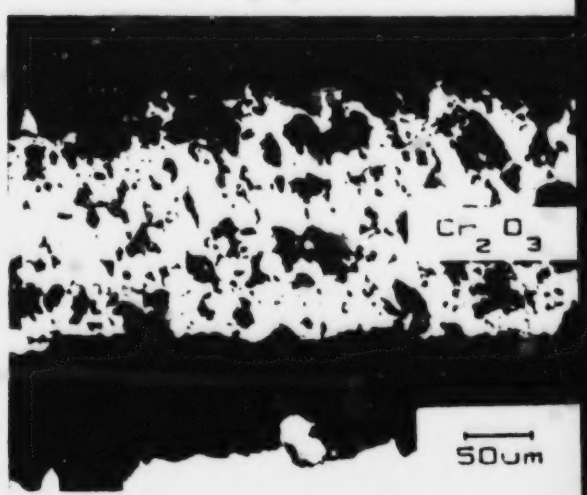

Figure 10b) - Metallographic cross-section of Cr_2O_3 coating after 1000 hours of salt spray exposure.

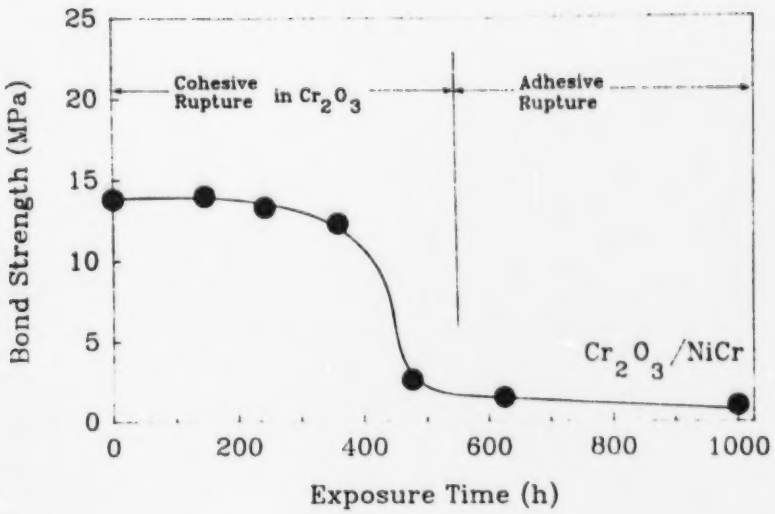

Figure 11a) - Bond strength of Cr_2O_3/NiCr coating as a function of corrosion time.

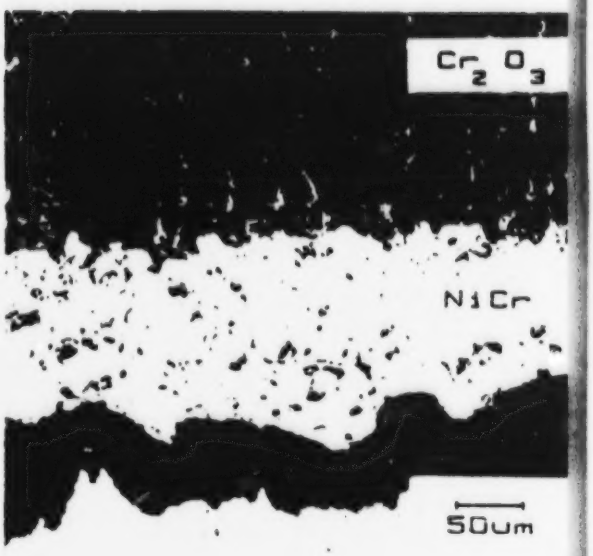

Figure 11b) - Metallographic cross-section of Cr_2O_3/NiCr coating after 1000 hours of salt spray exposure.

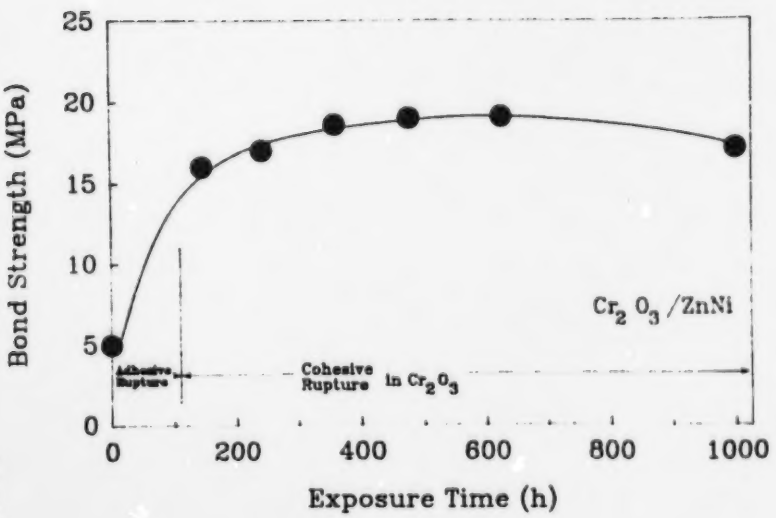

Figure 12a) - Bond strength of Cr_2O_3/ZnNi coating as a function of corrosion time.

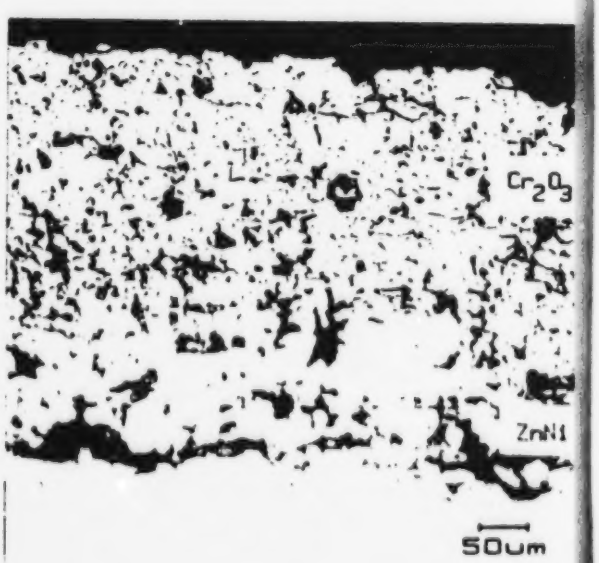

Figure 12b) - Metallographic cross-section of Cr_2O_3/ZnNi coating after 1000 hours of salt spray exposure.

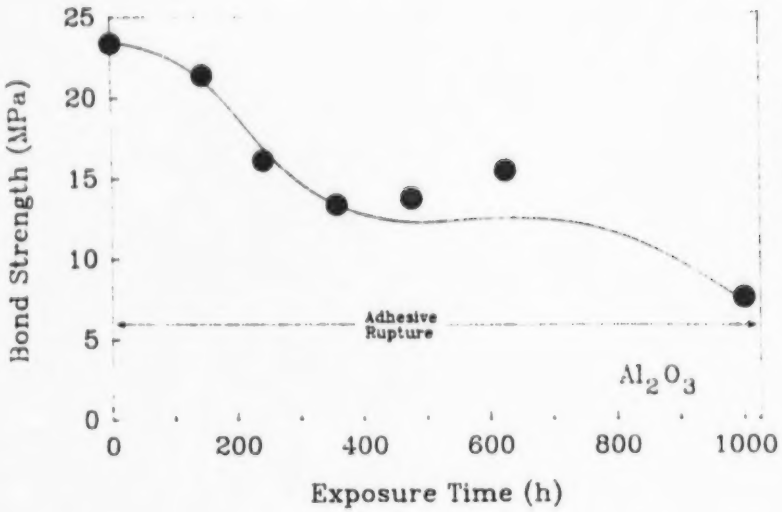

Figure 13a) - Bond strength of $Al_2O_3.TiO_2$ coating as a function of corrosion time.

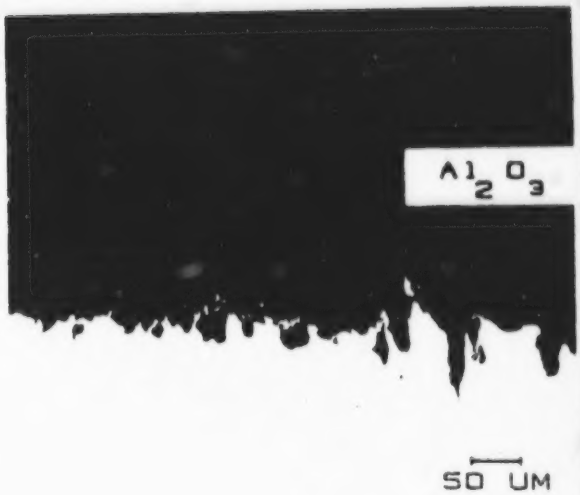

Figure 13b) - Metallographic cross-section of $Al_2O_3.TiO_2$ coating after 1000 hours of salt spray exposure.

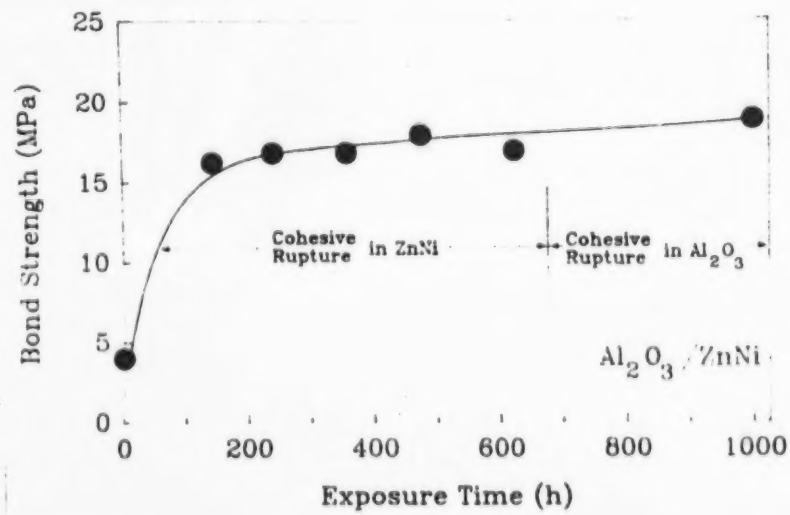

Figure 14a) - Bond strength of $Al_2O_3.TiO_2$/ZnNi coating as a function of corrosion time.

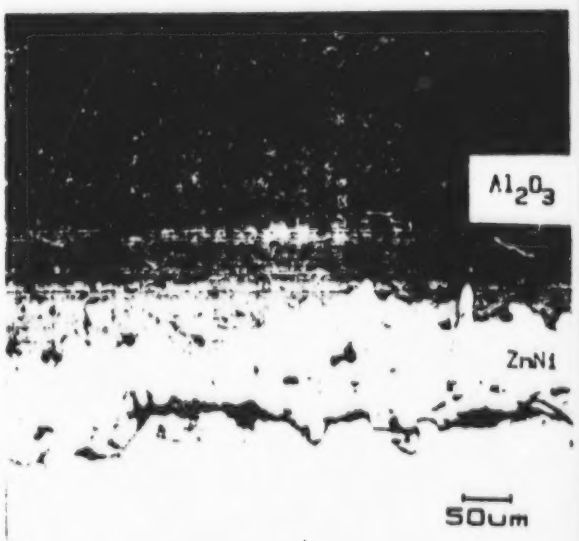

Figure 14b) - Metallographic cross-section of $Al_2O_3.TiO_2$/ZnNi coating after 1000 hours of salt spray exposure.